Excited State Processes in Supramolecular Complexes of Cyclic Dibenzopyrrolopyrrole Isomers with C$_{60}$ Fullerene

Gibu George,[a] Olga. A. Stasyuk,[a] Alexander A. Voityuk,[a] Anton J. Stasyuk,*[a, b] and Miquel Solà*[a]

Abstract: An approach to modulating the properties of carbon nanorings by incorporating pyrrolo[3,2-b]pyrrole units is of particular interest due to the combined effect of heteroatom and antiaromatic character on electronic properties. The inclusion of units other than phenylene leads to the formation of stereoisomers. In this work, we computationally study how the spatial orientation of monomeric units in the ring affects the properties of cyclic dibenzopyrrolo[3,2-b]pyrroles and their complexes with **C$_{60}$** fullerene. For **[4]PP** and **[4]DHPP**, the most symmetrical AAAA isomer is the most stable and forms stronger interactions with fullerene than the isomers where one or two monomeric units are flipped, mostly due to less Pauli repulsion. π-Electron delocalization in the monomeric unit is crucial for directing the electron transfer (from or to nanoring). The energy of excited states with charge transfer depends on the HOMO–LUMO gap, which varies from one stereoisomer to another only for **[4]DHPP⊃C$_{60}$** with aromatic 1,4-dihydropyrrolo[3,2-b]pyrrole units. The rates of electron transfer and charge recombination reactions are relatively weakly dependent of the spatial isomerism of nanorings.

Introduction

The first rational synthesis of cycloparaphenylenes (CPPs) was made by Bertozzi and co-workers in 2008.[1] Over the next few years, numerous syntheses of other nanorings and their derivatives were carried out.[2–5] Synthetic advances of the last decade allowed to construct CPPs with precise number of phenylene units. CPPs with 5-to-18 phenylene units are currently known. Due to interesting structure and remarkable optoelectronic properties, CPPs have attracted a lot of attention from chemists and material scientists.[6–8] Among the most unusual properties of CPPs are their size-dependent properties of emission but invariance of absorption.[9,10] However, changing the size is not the only way to modulate the properties of nanorings. The most obvious approach is to introduce units other than benzene. Incorporation of heteroaromatic or poly-aromatic units with donating or withdrawing properties made it possible to dramatically enrich the chemistry of nanorings, modifying their structural and optoelectronic properties.[11–13]

A new approach to modulating the properties of nanorings is the replacement of benzene rings with antiaromatic units as proposed by Prof. Esser. The first example of a nanoring with antiaromatic units was synthesized in 2020. Esser and co-workers incorporated two dibenzo[a,e]pentalene (DBP) units into [12]cycloparaphenylenes ([12]CPP).[14] Optoelectronic measurements showed an ambipolar electrochemical behavior of the nanorings due to the presence of the DBP and six phenyl linkers. Later, the nanorings containing different number of DBP units or even exclusively build from DBP units were reported.[15] The size and round shape of [4]DBP make it possible to effectively accommodate C$_{60}$ and C$_{70}$ fullerenes. The binding constant for [4]DBP⊃C$_{60}$ in toluene was found to be (1.35 ± 0.03)·10^5 M^{-1}.[15] The authors demonstrated that incorporating antiaromatic units into nanorings making them attractive as potential electronic materials.[16]

It is known that heteroatoms in a carbon π-conjugated system can drastically change its properties.[17–19] Doping with nitrogen or boron atoms changes the band structure of organic molecules, thereby modulating their semiconductor and luminescent properties.[20–22] Nitrogen atoms in antiaromatic hydrocarbons increase their electron-withdrawing ability.[23] Therefore, changing electronic properties of nanoring by heteroatom doping can serve as a convenient tool for tuning their optoelectronic properties in donor-acceptor complexes with fullerene.

[a] G. George, Dr. O. A. Stasyuk, Prof. A. A. Voityuk, Dr. A. J. Stasyuk, Prof. M. Solà
Institut de Química Computacional i Catàlisi and
Departament de Química
Universitat de Girona
C/ Maria Aurèlia Capmany 69, 17003 Girona, Catalonia (Spain)
E-mail: miquel.sola@udg.edu
        anton.stasyuk@udg.edu

[b] Dr. A. J. Stasyuk
Faculty of Chemistry
University of Warsaw
Pasteura 1, 02-093 Warsaw (Poland)

Chemistry–A European Journal

Research Article
doi.org/10.1002/chem.202300503

Chemistry
Europe
European Chemical
Societies Publishing

We have recently demonstrated that the cyclic tetramers of benzene-fused aromatic 1,4-dihydropyrrolo[3,2-b]pyrrole ([4]DHPP) and antiaromatic pyrrolo[3,2-b]pyrrole ([4]PP) are capable of accommodating C_{60} fullerene. According to the DFT results obtained with the Tamm-Dancoff approximation (TDA), such complexes show different behavior upon photoexcitation, depending on the degree of aromaticity of the nanoring. In particular, the electron transfer in [4]DHPP⊃C_{60} occurs from the nanoring to C_{60}, while in [4]PP⊃C_{60} the electron transfer from C_{60} to [4]PP is almost barrierless and characterized by ultrafast kinetics.[24]

In this work, we report a theoretical study of electronic and photoinduced electron transfer (PET) properties of the [4]DHPP⊃C_{60} and [4]DHPP⊃C_{60} complexes. We study in detail how electronic structure of monomeric units of the [4]PP and [4]DHPP nanorings and their mutual orientation affect the ground and excited state properties of inclusion complexes.

Results and Discussion

Ground state properties

Nanoring built from DHPP or PP units can exist in several diastereomeric forms. Such stereoisomers can be generated by rotating one or more monomeric units around single C–C bonds (Figure 1). We have recently demonstrated that stereo-isomers of Ir-based half-sandwich [60]fullerene complexes exhibit stereospecificity towards photoinduced electron transfer.[25] To understand the behavior of the [4]DHPP and [4]PP nanorings, 4 possible stereoisomers of each nanoring were considered. Geometries of the stereoisomers were optimized using the BLYP-D3(BJ)/def2-SVP level of theory.[26–29] These ground state geometries were used for the rest of calculations. The energies of the BLYP-D3(BJ)/def2-SVP optimized species were refined using the def2-TZVP basis set (see

Supporting Information). We compared relative stability of the [4]PP isomers using the BLYP and range-separated CAM-B3LYP, ωB97X-V, and M11 functionals to check for the influence of self-interaction error and incorrect description of long-range correlation effects[30–32] (Table S1, Supporting Information). All tested functionals, including BLYP, show the same stability order of isomers.

For both nanorings, the most symmetrical AAAA isomer turned out to be the most stable in the ground state (GS). It is important to note that all isomers lie in a small energy range, less than 1.6 kcal/mol for [4]DHPP and less than 2.0 kcal/mol for [4]PP. The stability of the two most stable isomers (AAAA and AABA) and the possibility of their transition into each other were evaluated by the energy barriers of the rotation of the monomer unit around the single C–C bond. These barriers are relatively high and equal to 25.55 and 28.30 kcal/mol at the BLYP-D3(BJ)/def2-TZVP level and 26.32 and 28.54 kcal/mol at the CAM-B3LYP-D3(BJ)/def2-TZVP level for DHPP and PP units, respectively (Figure S1, Supporting Information). Thus, the formation of one or another isomer is mainly determined by the synthetic path.

In addition, the aromaticity/antiaromaticity of the mono-mers was analyzed for the different isomers of [4]DHPP/[4]PP using the HOMA index.[33,34] According to the results, the HOMA values vary only slightly, being somewhat higher in the flipped units B (Table S2, Supporting Information). Minor differences in HOMA values can be explained by very small changes in the geometry of the monomeric units when moving from one isomer to another.

Structural similarity of the considered nanorings with the experimentally reported cyclic DBP tetramer suggests that [4]DHPP and [4]PP can also act as host for C_{60} fullerene. We investigated the electronic properties of the inclusion complexes (Figure 2) and compared their response to the photo-excitation depending on the relative orientation of the mono-meric units in the [4]DHPP and [4]PP nanorings.
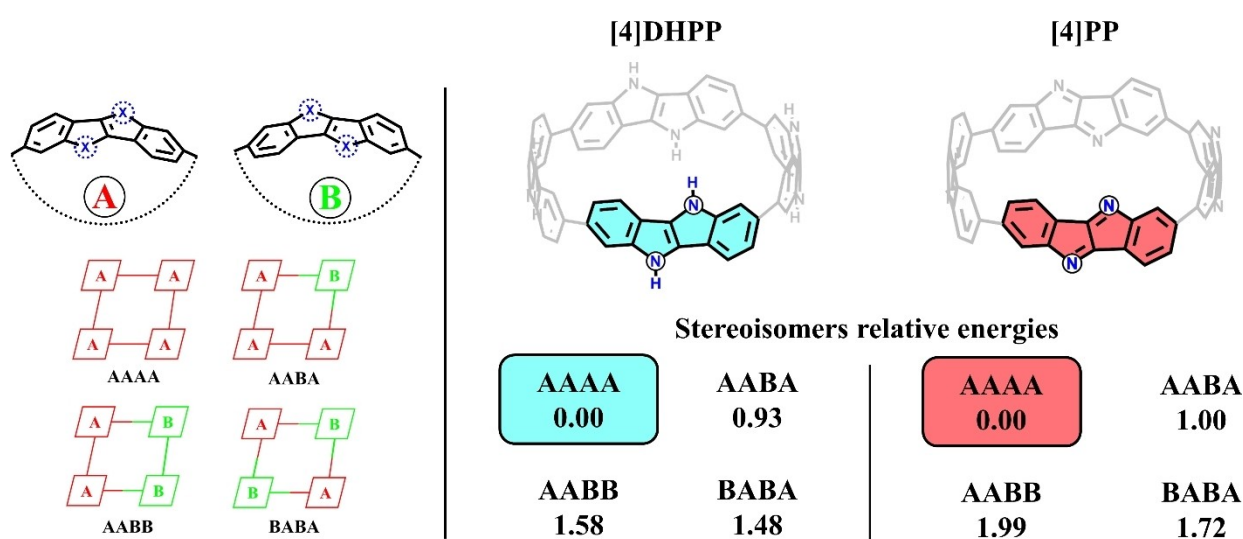

Figure 1. Structures of [4]DHPP and [4]PP nanorings as well as ground state relative energies (in kcal/mol) of their stereoisomers, calculated at BLYP-D3(BJ)/def2-TZVP.
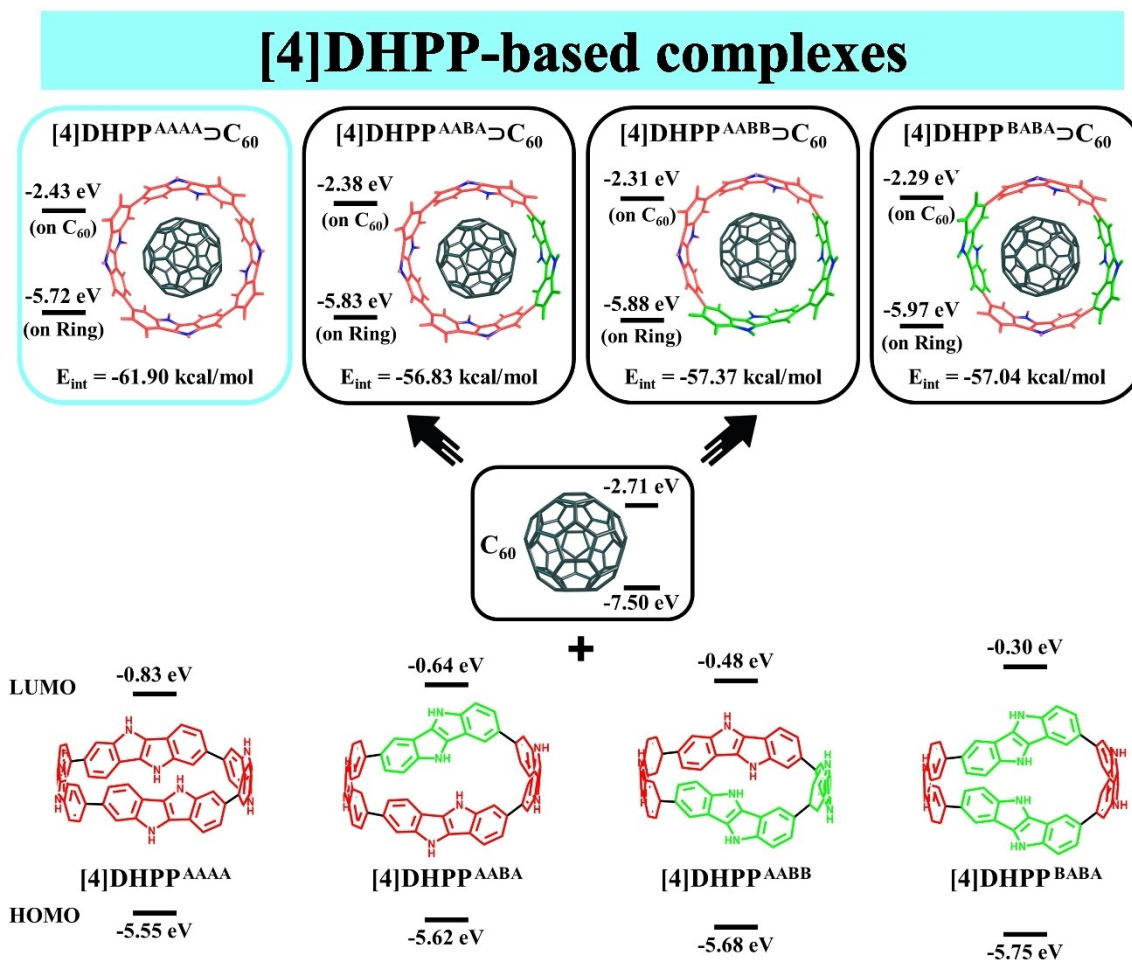
Chemistry–A European Journal

Research Article
doi.org/10.1002/chem.202300503

Chemistry Europe
European Chemical
Societies Publishing

Figure 2. HOMO and LUMO energies (in eV, CAM-B3LYP/def2-SVP) of [4]DHPP⊃C_{60} stereoisomers and their subunits.

First, we analyzed the orbital energies of the [4]DHPP⊃C_{60} and [4]PP⊃C_{60} complexes and their individual fragments obtained at the CAM-B3LYP/def2-SVP level. As seen in Figure 2, the HOMO and LUMO energies of [4]DHPP and the corresponding inclusion complexes show a noticeable shift when going from one stereoisomer to another. [4]DHPP^{AAAA} has an energy gap of 4.72 eV, which is the smallest among the isomers. When going from AAAA to BABA isomers, the band gap increases and riches its maximum value of 5.45 eV for [4]DHPP^{BABA}. Important to note that in all [4]DHPP⊃C_{60} stereoisomers, the HOMO orbital is localized on the nanoring, being more stable in the BABA isomer. In turn, the LUMO is localized on C_{60}, and its destabilization was observed moving to BABA.

In contrast to [4]DHPP, no significant changes in orbital energies were found for different stereoisomers of [4]PP. The HOMO energies were found to be −7.08 eV, while the LUMOs fluctuate in a narrow energy range, from −2.74 to −2.76 eV. The formation of [4]PP⊃C_{60} complexes leads to an insignificant (about 0.1 eV) shift in the LUMO energy, which is localized on the nanoring. The HOMO of the [4]PP⊃C_{60} complexes is localized on C_{60} and its energy does not change when the structure of the complex changes (Figure 3). Important to note

that the much lower LUMOs of the [4]PP nanorings with antiaromatic fragments suggest that they should be much stronger electron acceptors compared to [4]DHPP with aromatic units.

We performed an analysis of the frontier molecular orbitals to understand the observed differences in the electronic nature of [4]DHPP and [4]PP. In the AAAA isomer of both nanorings, the contribution of the atomic orbitals (AOs) to the HOMO and LUMO is uniformly delocalized between all four units. However, the rotation of one of the monomeric unit through the nanoring and generation of the AABA isomer has fundamentally different effect on the orbital lobes distribution. In the case of [4]DHPP, the rotated unit B is almost completely excluded from the HOMO and LUMO. At the same time, in the [4]PP nanoring, such rotation does not lead to a significant redistribution of the AOs contributions to HOMO and LUMO (Figure 4). A similar picture is observed for other stereoisomers. In the AABB isomer of [4]DHPP, both rotated units are not involved in the HOMO and LUMO, while in [4]PP, the orbital lobes are still located on the rotated fragments.

In addition, the change in the orbital energies is different during the formation of the complexes with fullerene. As seen
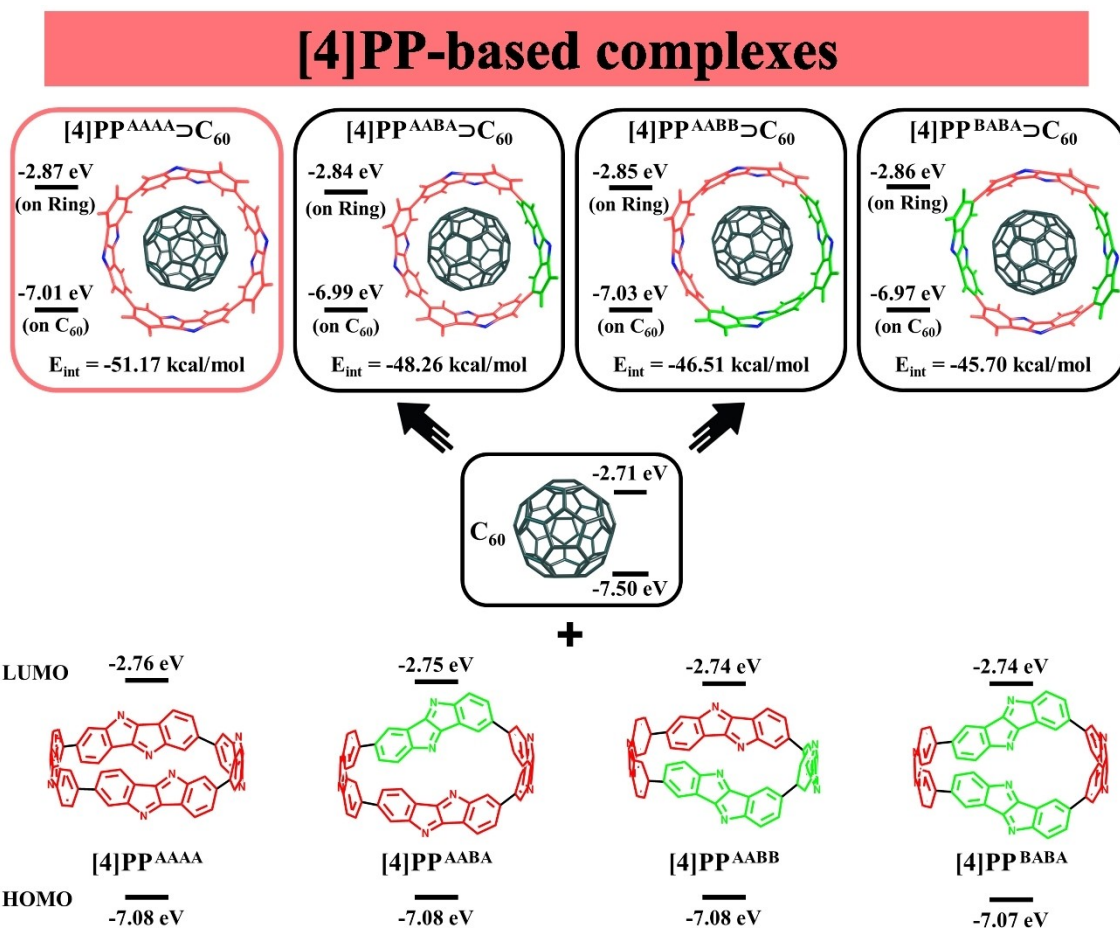
Chemistry–A European Journal

Research Article
doi.org/10.1002/chem.202300503

Chemistry
Europe
European Chemical
Societies Publishing

Figure 3. HOMO and LUMO energies (in eV, CAM-B3LYP/def2-SVP) of [4]PP⊃C$_{60}$ stereoisomers and their subunits.
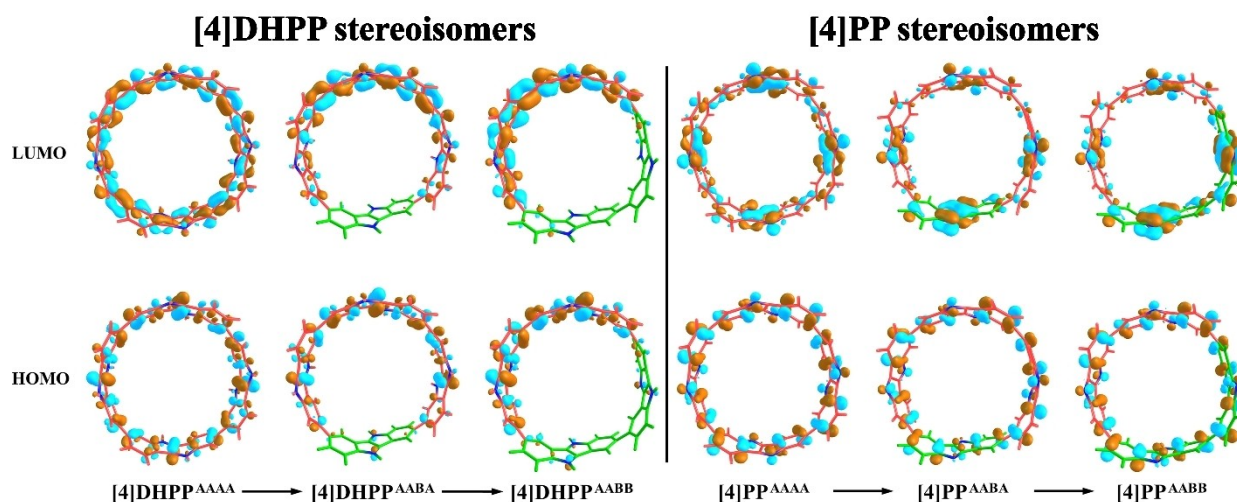
Figure 4. HOMO and LUMO shapes for AAAA, AABA, and AABB stereoisomers of [4]DHPP and [4]PP.

in Figure 2, the formation of the [4]DHPP⊃C$_{60}$ complexes results in the stabilization of the HOMOs localized on nanorings by ca. 0.2 eV, while the energy of LUMOs localized on C$_{60}$ increases by 0.3–0.4 eV. The observed shift can be associated with a partial charge transfer between fullerene cage and nanoring in the ground state. The analysis performed within the framework of the most popular charge partitioning schemes (Table S3, Supporting Information) reveals a partial charge

Chemistry–A European Journal

Research Article
doi.org/10.1002/chem.202300503

Chemistry Europe
European Chemical
Societies Publishing

transfer. Depending on the population scheme, the maximal amount of the transferred charge varied from 0.08 to 0.22 e for [4]DHPP⊃C_{60} complexes. In contrast, in the [4]PP⊃C_{60} complexes, this value does not exceed 0.08 e (Table S3, Supporting Information). Important to note that in all [4]DHPP⊃C_{60} complexes the charge was transferred from nanorings to C_{60}.

To estimate the stability of the complexes, the interaction energy (ΔE_{int}) between C_{60} and nanorings was computed. For [4]DHPP⊃C_{60}, ΔE_{int} at the BLYP-D3(BJ)/TZ2P level is in the range from −61.9 to −57.0 kcal/mol, while for [4]PP⊃C_{60}, ΔE_{int} varies from −51.2 to −45.7 kcal/mol, depending on the stereoisomer of nanoring. A general trend in the stability of complexes remained the same, when the BLYP functional was replaced by CAM-B3LYP (Table S4, Supporting Information). In addition, we performed an energy decomposition analysis (EDA) of the ΔE_{int} using the Morokuma-like scheme[35,36] to find a reason of their different stability (Table 1). The EDA decomposes the interaction energy into four components: electrostatic (ΔE_{elstat}), Pauli repulsion (ΔE_{Pauli}), orbital interactions (ΔE_{oi}), and dispersion corrections (ΔE_{disp}), and allows one to estimate the nature of interactions.

Despite the similar nature of the non-covalent interactions, [4]DHPP isomers form stronger complexes with C_{60} fullerene than [4]PP isomers, most likely due to more suitable size complementarity. According to Table 1, among the attracting terms ($\Delta E_{elstat} + \Delta E_{oi} + \Delta E_{disp}$), the dispersion is the dominant one, with a contribution of about 50%. The second largest term is the electrostatic attraction with a contribution of about 33–35%. The orbital interactions provide only 14–16% of the total stabilization interactions. It is important to emphasize that the Pauli repulsion increases when moving from the most symmetrical AAAA conformer to the BABA conformer. However, an increase in the attractive interactions, especially ΔE_{oi} and ΔE_{disp}, suggests that the energy changes are associated with a decrease of the geometrical size of nanoring. We compared the effective radii of different stereoisomers of [4]DHPP and [4]PP in their complexes with fullerene (Figure S2 and S3) and found a similar trend for them. The radius of nanoring in [4]DHPP⊃C_{60} varies from 6.52 Å for the AAAA isomer to 6.40 Å for the BABA one, whereas in [4]PP⊃C_{60}, the radius changes from 6.48 Å to 6.39 Å. Thus, the smaller size of the nanorings is responsible for

weaker interactions because of stronger Pauli repulsion, especially in the case of BABA isomers.

The host–guest interaction topology was analyzed using electron density, its Laplacian at the bond critical points (BCPs) and other topological parameters from QTAIM (see Table S5).[37] In all complexes, only π⋯π interactions between host and guest units were detected. The number of BCPs depends on the stereoisomer of the nanoring. In general, the [4]DHPP⊃C_{60} complexes with aromatic units are characterized by a larger number of BCPs (22–23) than the [4]PP⊃C_{60} complexes (18–20). Taking into account that the characteristics of BCPs are quite similar for [4]DHPP⊃C_{60} and [4]PP⊃C_{60} (Table S5), the greater number of BCPs found in [4]DHPP⊃C_{60} correlates well with their higher stability compared to [4]PP⊃C_{60}. The QTAIM molecular graphs are given in Figures S4 and S5, Supporting Information.

Singlet excited states

Taking into account the different electronic properties of [4]DHPP and [4]PP, as well as their dependence on the mutual orientation of monomeric units, it can be expected that the fullerene inclusion complexes will behave differently upon photoexcitation. Simulations of the excited states were performed using the TDA-DFT method with the CAM-B3LYP-D3(BJ)/def2-SVP scheme. Table S7 shows that the energies of LE and CT states for the AAAA isomer of [4]DHPP⊃C_{60} obtained at the CAM-B3LYP/def2-SVP and CAM-B3LYP/def2-TZVP levels of theory differ by less than 0.1 eV.[28,29,38] Contributions of the C_{60} guest and the [4]DHPP/[4]PP hosts to the excited state electronic density were analyzed for the lowest 80 excited states of each complex. The excited states were classified into three groups: (1) locally excited (LE) states with excitation on one of fragments and very small charge separation, CS < 0.1 e; (2) charge transfer (CT) states with CS > 0.9 e between fragments, and (3) mixed states with 0.1 e < CS < 0.9 e.

In the gas phase, the 80 lowest vertical singlet excitation energies for the series of [4]DHPP⊃C_{60} complexes vary from 1.85 to 4.15 eV. Regardless of the [4]DHPP stereoisomer, the lowest excited state is a CT1 state, where electron density is transferred from [4]DHPP to C_{60} (Table 2). This CT state can

Table 1. Interaction energy (in kcal/mol) and its components[a] for [4]DHPP⊃C_{60} and [4]PP⊃C_{60} complexes, calculated at BLYP-D3(BJ)/TZ2P.

	ΔE_{Pauli}	ΔE_{elstat}	ΔE_{oi}	ΔE_{disp}	ΔE_{int}
			[4]DHPP⊃C_{60}		
AAAA	156.41	−70.88 (32.5%)	−32.34 (14.8%)	−115.09 (52.7%)	−61.90
AABA	181.60	−81.11 (34.0%)	−36.61 (15.4%)	−120.72 (50.6%)	−56.83
AABB	185.43	−83.47 (34.4%)	−39.32 (16.2%)	−120.01 (49.4%)	−57.37
BABA	207.03	−93.75 (35.5%)	−43.35 (16.4%)	−126.97 (48.1%)	−57.04
			[4]PP⊃C_{60}		
AAAA	168.95	−72.80 (33.1%)	−31.59 (14.4%)	−115.72 (52.6%)	−51.17
AABA	182.79	−77.44 (33.5%)	−34.71 (15.0%)	−118.89 (51.5%)	−48.26
AABB	188.44	−79.79 (34.0%)	−37.23 (15.8%)	−117.93 (50.2%)	−46.51
BABA	207.64	−88.47 (34.9%)	−40.55 (16.0%)	−124.32 (49.1%)	−45.70

[a] The percentage contributions to the sum of attracting terms ($\Delta E_{elstat} + \Delta E_{oi} + \Delta E_{disp}$) are given in parentheses.

Chemistry–A European Journal

Research Article
doi.org/10.1002/chem.202300503

Chemistry Europe
European Chemical
Societies Publishing

Table 2. Excitation energies (E_x, eV), main singly excited configuration (HOMO(H)–LUMO(L)) and its weight (W), oscillator strength (f), extent of charge transfer (CT, e) or localization of exciton (X) for [4]DHPP⊃C$_{60}$ and [4]PP⊃C$_{60}$ complexes in the gas-phase at CAM-B3LYP-D3(BJ)/def2-SVP.

	Supramolecular host–guest systems							
	[4]DHPP⊃C$_{60}$				[4]PP⊃C$_{60}$			
	AAAA	AABA	AABB	BABA	AAAA	AABA	AABB	BABA
	LE^{Guest} (Fullerene C$_{60}$)							
E_x	2.389	2.302	2.352	2.255	2.397	2.425	2.450	2.402
Transition (W)	H-4-L (0.58)	H-8-L+1 (0.17)	H-6-L (0.16)	H-8-L+2 (0.24)	H–L+4 (0.86)	H–L+4 (0.31)	H–L+3 (0.49)	H–L+4 (0.48)
f	<0.001	<0.001	<0.001	<0.001	<0.001	<0.001	<0.001	<0.001
X	0.905	0.868	0.874	0.861	0.912	0.837	0.865	0.847
	LE^{Host} ([4]DHPP/[4]PP nanoring)							
E_x	2.826	2.961	3.148	3.308	2.145	2.125	2.119	2.133
Transition (W)	H–L+6 (0.49)	H–L+6 (0.58)	H–L+6 (0.34)	H–L+6 (0.21)	H-1-L (0.31)	H-1-L (0.15)	H-1-L (0.14)	H-1-L (0.26)
f	0.002	0.094	0.132	0.027	0.012	0.008	0.008	0.003
X	0.901	0.890	0.842	0.825	0.950	0.917	0.910	0.857
	CT1 (nanoring→C$_{60}$)							
E_x	1.846	1.986	2.114	2.143	3.245	3.253	3.229	3.248
Transition (W)	H–L (0.97)	H–L (0.90)	H–L (0.44)	H–L (0.71)	H-1-L+3 (0.41)	H-3-L+1 (0.17)	H-3-L+1 (0.22)	H-4-L+4 (0.31)
f	0.001	0.001	0.001	0.005	<0.001	0.008	0.044	0.015
CT	0.971	0.958	0.964	0.926	0.917	0.801	0.831	0.856
	CT2 (C$_{60}$→nanoring)							
E_x	n/a[a]	n/a[a]	n/a[a]	n/a[a]	2.471	2.508	2.426	2.466
Transition (W)					H–L (0.42)	H–L (0.68)	H–L (0.37)	H–L (0.36)
f					0.004	0.013	0.005	0.012
CT					0.909	0.824	0.799	0.807

[a] States of interest are not found within the 80 lowest excited states.

largely be described as a HOMO–LUMO transition with more than 0.9 e transferred. Its energy depends on the isomer of the nanoring, being almost 0.3 eV higher for the BABA stereoisomer than for AAAA. The LE^{Guest} state (localized on C$_{60}$) is fairly the same for all complexes and was found around 2.3 eV. However, the energies of the LE^{Host} (localized on nanoring) changes when moving from AAAA to BABA isomer. In particular, the LE^{Host} energy in the BABA isomer is almost 0.5 eV higher than in AAAA (3.31 and 2.83 eV, respectively). This is due to the significantly different delocalization of the electron density, as shown in Figure 4. π-electron delocalization over a smaller fragment of the [4]DHPP nanoring leads to a shift in absorption towards higher energies. The excited states corresponding to the electron transfer from C$_{60}$ to [4]DHPP were not found within the studied range of energies. Table 2 contains the data for the lowest-energy excited states of each type.

Analysis of the excited states of [4]PP⊃C$_{60}$ revealed that the range of energy from 2.12 to 3.95 eV is somewhat smaller than for [4]DHPP⊃C$_{60}$. In contrast to [4]DHPP⊃C$_{60}$, the lowest excited states of the [4]PP⊃C$_{60}$ complexes correspond to LE^{Host}, which lies 0.68 to 1.17 eV lower than the LE^{Host} in [4]DHPP⊃C$_{60}$. As expected, the energy of the LE^{Guest} in all systems is almost identical and does not depend on the electronic nature of the host nanoring. As can be seen in Figure 3, the energies of HOMO and LUMO for [4]PP are noticeably lower than the values for [4]DHPP, and very similar to the orbital energies of C$_{60}$. Thus, it can be suggested that [4]PP with antiaromatic units in the ring can exhibit pronounced electron-withdrawing properties, contrary to [4]DHPP with electron-donating properties. According to the computational results, in [4]PP⊃C$_{60}$ there are

two types of CT states. CT1 states with the electron density transferred from [4]PP to C$_{60}$ are 0.8 eV higher in energy compared to CT2 states with the electron transfer from C$_{60}$ to [4]PP nanorings.

Effects of environment

We used a COSMO-like model[39,40] with dichloromethane as a solvent to investigate how polar environment affects electronic excitations. The ground state (GS) solvation energy for the [4]DHPP⊃C$_{60}$ complexes is about −0.9 eV, while for the [4]PP⊃C$_{60}$ systems, this value is about −0.6 eV. For the various nanoring stereoisomers, the change in solvation energies does not exceed 0.01 eV for both systems. High ability of fragments to charge delocalization is reflected in the relatively small GS dipole moments of the complexes, which vary from 0.3 to 2.6 D and 0.3 to 0.5 D for [4]DHPP⊃C$_{60}$ and [4]PP⊃C$_{60}$, respectively. The difference between the dipole moments of the GS and LE states does not exceed 2.0 D for all complexes. Therefore, as expected, the solvation energies of the LE^{Host} and LE^{Guest} states are very similar to the energies of the GS. Detailed data on the solvation of the complexes are presented in Table S5, Supporting Information.

Typically, the solvation energies of the CT states are much higher than those of the GS or LE states due to the polarity of the systems. However, our previous investigations show that for fullerene complexes with various carbon-rich hosts, such as bowl-shaped molecules,[19] CPPs and their π-extended analogs, the solvation energy of the CT states is only slightly different

Chemistry–A European Journal

Research Article
doi.org/10.1002/chem.202300503

Chemistry
Europe
European Chemical
Societies Publishing

from the energy of the GS.[41–44] For the [4]DHPP⊃C_{60} complexes, a difference in the dipole moments ($\Delta\mu$) for CT1 and GS states was found in the range from 1.8 to 12.6 D. Taking into account that the GS→CT1 transition corresponds to the HOMO-to-LUMO transition, the observed range of the dipole moment changes is fully consistent with the HOMO localization on the [4]DHPP fragment. The minimum $\Delta\mu$ value corresponds to the most symmetrical AAAA isomer, while the maximum value correspond to the least symmetrical AABB isomer. The solvation energies of the CT1 states range from −0.90 to −1.02 eV.

Important to note that the CT1 is the only type of charge-separated state found in the [4]DHPP⊃C_{60} systems. Despite the similarity of solvation energies for the CT1 and LE^{Guest} states, the BABA isomer is characterized by a much smaller gap between these states than AAAA. In particular, it changes from 0.57 eV for AAAA to 0.15 eV for the BABA isomer. Nevertheless, the CT1 state in [4]DHPP⊃C_{60} remains the lowest excited state in the DCM solvent, regardless of the [4]DHPP isomer, and can probably be observed in spectroscopic experiment.

For the [4]PP⊃C_{60} complexes, the difference between GS and CT1 dipole moments varies from 4.2 to 5.2 D, depending on the particular [4]PP isomer. The similarity of $\Delta\mu$ values is reflected in the similarity of the CT1 solvation energies, which ranges from −0.72 to −0.75 eV. For the GS→CT2 transition, the solvation energies are much higher and range from −1.10 to −1.30 eV. Slightly higher solvation energy for the AAAA isomer compared to the others was observed due to the highest charge transfer values (Table 2). Solvation details are given in Table S6, Supporting Information. Worth mentioning that the stabilization of the CT2 state by the solvent turned out to be sufficient for all stereoisomers to rearrange this state with the LE states in DCM and to make the CT2 the lowest excited state. In turn, the stabilization of the CT1 is rather weak, and this state remains higher in energy than LE^{Guest} and LE^{Host} states. Thus, for [4]PP⊃C_{60} complexes, only the electron transfer from C_{60} to [4]PP can be observed experimentally.

Electron transfer rates

The data in Table 2 show that the GS→CT transitions are characterized by a very weak oscillator strength for all complexes. It means that direct population of the CT states after light absorption has a low probability. Thus, we have considered the decay of both LE^{Guest} and LE^{Host} states as the main channel for generating states with electron transfer (ET). The semi-classical method[45] by Ulstrup and Jortner was used to calculate the rates of electron transfer (k_{ET}) and charge recombination (k_{CR}). The important parameters that control k_{ET} and k_{CR} rates in DCM are listed in Table 3 (for [4]DHPP⊃C_{60}) and Table 4 (for [4]PP⊃C_{60}). The fragment charge difference (FCD) method[46] was employed to calculate the electronic couplings in this work.

According to the results, the electron transfer in all [4]DHPP⊃C_{60} complexes is thermodynamically favorable, i.e. proceeds with negative Gibbs energy. The decay of the LE^{Host} states to the CT1 state occurs in the inverted Marcus region ($|\Delta G^0| > \lambda$). In turn, the decay of the LE^{Guest} states takes place in the normal Marcus region ($|\Delta G^0| \leq \lambda$, except for the AAAA conformer) and slightly faster than the decay of the LE^{Host} states. The assignment of the process to the inverted or normal region was made in accordance with the classical Marcus theory. The rate of electron transfer increases with driving force until the reorganization energy matches the driving force ($-\Delta G^0 = \lambda$) and then becomes slower for more negative ΔG^0. The calculated k_{ET} values are in a good agreement with experimentally reported data for fullerene based complexes of π-extended nanorings.[47] Interesting to note that the electron transfer process in the complexes of AABB and BABA isomers is 2–6 times faster than in AAAA and AABA.

As mentioned above, two types of CT states were found for the [4]PP⊃C_{60} complexes. Generation of the CT1 state with [4]PP→C_{60} electron transfer is very unlikely by the decay of both LE^{Guest} and LE^{Host} due to highly positive Gibbs energy of this process (Figure 5). In turn, the formation of the CT2 state, where fullerene acts as electron donor, is thermodynamically

Table 3. Gibbs energy ΔG^0 (in eV), electronic coupling $|V_{ij}|$ (in eV), reorganization energy λ (in eV), activation energy E_a (in eV), and rates k_X (in s^{-1}) for ET and CR processes in [4]DHPP⊃C_{60} calculated in DCM.

Conformer	Transition	$\Delta G^{0[a]}$	$|V_{ij}|$	λ	E_a	k_x
				Electron transfer (LE→CT)		
AAAA	LE^{Guest}→CT1	−0.573	$1.96 \cdot 10^{-3}$	0.376	0.012	$3.60 \cdot 10^{10}$
	LE^{Host}→CT1	−1.000	$6.58 \cdot 10^{-3}$	0.367	0.015	$3.05 \cdot 10^{10}$
AABA	LE^{Guest}→CT1	−0.385	$4.22 \cdot 10^{-3}$	0.456	0.016	$9.01 \cdot 10^{10}$
	LE^{Host}→CT1	−1.045	$3.10 \cdot 10^{-3}$	0.446	0.016	$4.98 \cdot 10^{10}$
AABB	LE^{Guest}→CT1	−0.382	$7.07 \cdot 10^{-3}$	0.525	0.017	$1.28 \cdot 10^{11}$
	LE^{Host}→CT1	−1.172	$3.32 \cdot 10^{-3}$	0.507	0.018	$3.98 \cdot 10^{10}$
BABA	LE^{Guest}→CT1	−0.146	$2.77 \cdot 10^{-3}$	0.506	0.002	$2.07 \cdot 10^{11}$
	LE^{Host}→CT1	−1.199	$6.41 \cdot 10^{-3}$	0.498	0.013	$3.80 \cdot 10^{10}$
				Charge recombination (CT→GS)		
AAAA	CT1→GS	−1.824	$2.38 \cdot 10^{-2}$	0.311	0.024	$2.35 \cdot 10^{7}$
AABA	CT1→GS	−1.943	$8.79 \cdot 10^{-3}$	0.309	0.028	$2.56 \cdot 10^{7}$
AABB	CT1→GS	−1.987	$3.24 \cdot 10^{-2}$	0.348	0.035	$4.31 \cdot 10^{7}$
BABA	CT1→GS	−2.131	$2.89 \cdot 10^{-2}$	0.294	0.027	$1.66 \cdot 10^{7}$

[a] Gibbs energy difference between the denoted states in DCM.

Chemistry–A European Journal

Research Article
doi.org/10.1002/chem.202300503

Chemistry
Europe
European Chemical
Societies Publishing

Table 4. Gibbs energy ΔG^0 (in eV), electronic coupling $|V_{ij}|$ (in eV), reorganization energy λ (in eV), activation energy E_a (in eV), and rates k_X (in s^{-1}) for ET and CR processes in **[4]PP⊃C$_{60}$** complexes calculated in DCM.

Conformer	Transition	$\Delta G^{0[a]}$	$|V_{ij}|$	λ	E_a	k_x
				Electron transfer (LE→CT)		
AAAA	LE^{Guest}→CT2	−0.615	$1.34\cdot10^{-2}$	0.309	0.013	$9.53\cdot10^{11}$
	LE^{Host}→CT2	−0.243	$1.71\cdot10^{-2}$	0.307	0.015	$9.58\cdot10^{12}$
AABA	LE^{Guest}→CT2	−0.420	$1.23\cdot10^{-2}$	0.357	0.016	$2.17\cdot10^{12}$
	LE^{Host}→CT2	−0.008	$1.55\cdot10^{-2}$	0.370	0.035	$2.58\cdot10^{12}$
AABB	LE^{Guest}→CT2	−0.480	$1.37\cdot10^{-2}$	0.408	0.014	$2.35\cdot10^{12}$
	LE^{Host}→CT2	−0.038	$1.60\cdot10^{-2}$	0.417	0.018	$7.25\cdot10^{12}$
BABA	LE^{Guest}→CT2	−0.399	$1.19\cdot10^{-2}$	0.438	0.015	$2.20\cdot10^{12}$
	LE^{Host}→CT2	−0.036	$1.77\cdot10^{-2}$	0.444	0.022	$5.71\cdot10^{12}$
				Charge recombination (CT→GS)		
AAAA	CT2→GS	−1.790	$1.73\cdot10^{-2}$	0.268	0.019	$9.78\cdot10^{6}$
AABA	CT2→GS	−1.982	$1.82\cdot10^{-2}$	0.282	0.018	$1.82\cdot10^{6}$
AABB	CT2→GS	−1.950	$1.51\cdot10^{-2}$	0.274	0.014	$2.22\cdot10^{6}$
BABA	CT2→GS	−1.983	$1.63\cdot10^{-2}$	0.294	0.018	$2.45\cdot10^{6}$

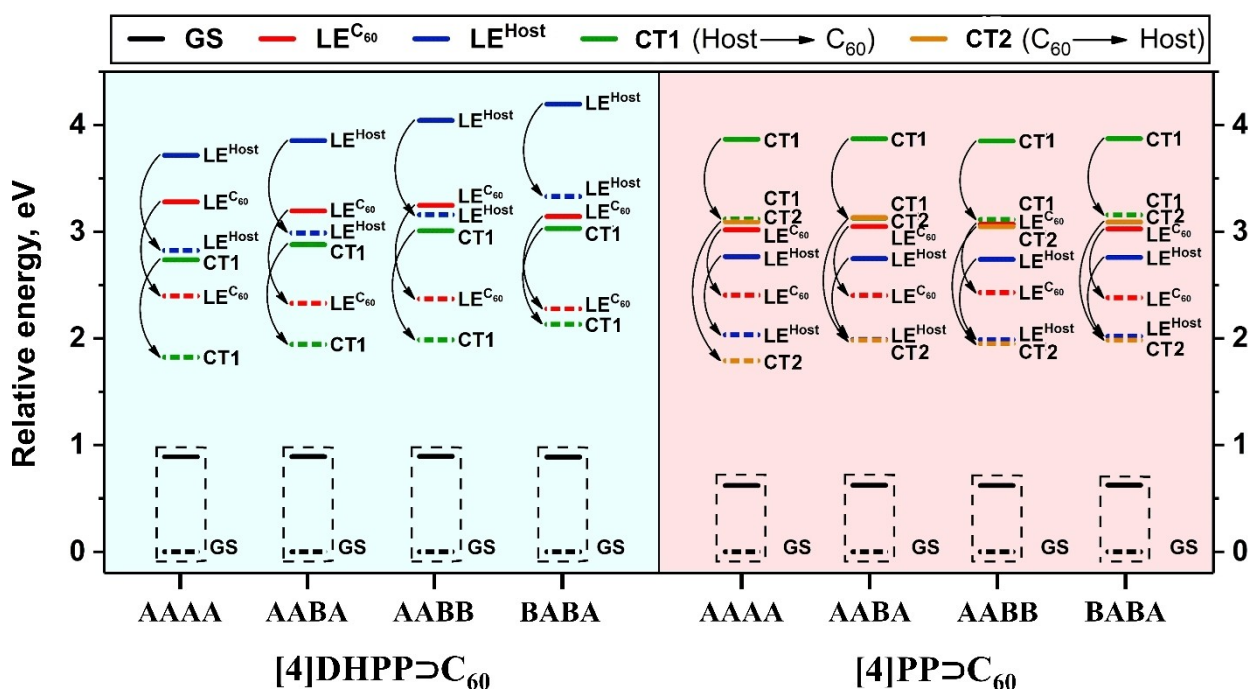[a] Gibbs energy difference between the denoted states in DCM.

Figure 5. Energies of LE and CT states in **[4]DHPP⊃C$_{60}$** and **[4]PP⊃C$_{60}$** in vacuum (solid lines) and dichloromethane (dash lines).

favorable from both LE^{Host} and LE^{Guest} states. This process occurs in the normal Marcus region (except the LE^{Guest}→CT2 reaction for AAAA isomer) with rather small activation energies. In all cases, the reaction was found to be ultrafast, in particular occurring in a few picoseconds.

In contrast, the charge recombination process, i.e. the decay of CT state to the GS, is significantly slower than the corresponding electron transfer in both **[4]DHPP** and **[4]PP** based complexes. The competition between electron transfer (or charge separation) and charge recombination is crucial for generation of a long-lived CT state and efficiency of a potential photovoltaic device. Thus, it can be concluded that the **[4]PP ⊃C$_{60}$** complexes with unusual electron transfer from fullerene

to nanoring are better suited for practical use because of ultrafast generation of the CT state and slow recombination of holes and electrons. Note that the rates of ET and CR processes were computed in the Franck-Condon region. We have previously shown that the effect of internal geometry reorganization on ΔG^0 is rather small for large conjugated systems such as fullerenes and their inclusion complexes.[48,49] The use of the FCD model, based on the unitary transformation of adiabatic states into diabatic ones, makes it possible to estimate the coupling beyond the crossing point. The FCD method provides good estimates of the coupling and is recommended for extended molecular systems.[50]

Chemistry–A European Journal

Research Article
doi.org/10.1002/chem.202300503

Chemistry Europe
European Chemical
Societies Publishing

Table 5. Rate of radiative decay of LE^{Host} state in [**4**]DHPP⊃C$_{60}$ and [**4**]PP⊃C$_{60}$ calculated in DCM. ΔE (in eV) is the energy difference between LE^{Host} and GS states, f – oscillator strength and k_x (in s^{-1}) is rate of radiative decay.

Conformer	[**4**]DHPP⊃C$_{60}$			[**4**]PP⊃C$_{60}$		
	ΔE	f	k_x	ΔE	f	k_x
			Radiative decay of LE^{Host} (LE^{Host}→GS)			
AAAA	2.824	0.002	$6.92 \cdot 10^5$	2.033	0.012	$2.15 \cdot 10^6$
AABA	2.988	0.094	$3.64 \cdot 10^7$	1.990	0.008	$1.37 \cdot 10^6$
AABB	3.159	0.132	$5.72 \cdot 10^7$	1.988	0.008	$1.37 \cdot 10^6$
BABA	3.330	0.027	$1.30 \cdot 10^7$	2.019	0.003	$5.31 \cdot 10^5$

Despite the fact that in all cases, electron transfer occurs much faster than the corresponding charge recombination process, the radiative decay of the LE^{Host} state can be considered as an alternative deactivation channel that prevents the formation of the CT state.

However, as can be seen in Table 5, the rate of such a process does not exceed 10^8 s^{-1} for any of the studied complexes, which is much slower than the electron transfer rate. Thus, radiative decay will not compete with the charge separation reaction and interfere with the generation of CT states.

Conclusions

We described here a series of supramolecular complexes of the [**4**]DHPP/[**4**]PP nanorings containing aromatic/antiaromatic fragments. Computational results revealed four stable stereo-isomers for each nanoring formed by rotation around single C–C bonds between monomeric units. The most stable isomer in the ground state is the most symmetrical one. The relative energies of other isomers are within 2 kcal/mol, while the rotational barrier is high. Host–guest interaction energy in supramolecular complexes of [**4**]DHPP with C$_{60}$ fullerene is higher than in [**4**]PP⊃C$_{60}$ complexes by *ca.* 10 kcal/mol, mainly due to more suitable size complementarity and less Pauli repulsion.

TDA-DFT calculations showed that the electron transfer upon photoexcitation of the host–guest complexes with C$_{60}$ fullerene is determined by the electronic nature of the nanoring. In particular, in [**4**]DHPP⊃C$_{60}$ with aromatic units, the only electron transfer from the nanoring to C$_{60}$ was found. In contrast, in [**4**]PP⊃C$_{60}$ containing antiaromatic fragments, such direction of the electron transfer is unlikely. However, due to significant lowering of the LUMO energies compared to [**4**]DHPP⊃C$_{60}$, the electron transfer from C$_{60}$ to [**4**]PP is almost barrierless and ultrafast.

The energy of the lowest CT states computed by the TDA-DFT method correlates with the HOMO–LUMO gap. Spatial orientation of the monomers changes the electron density distribution at HOMO of the [**4**]DHPP nanoring, providing slightly better electron-donating properties for the AAAA isomer. A blue shift of the CT1 state by 0.3 eV was found comparing the AAAA and BABA stereoisomers of [**4**]DHPP⊃C$_{60}$. In turn, [**4**]PP isomers show almost the same HOMO and LUMO energies; therefore, the electron transfer characteristics of its complex with fullerene do not depend on the nanoring isomer.

Efficient charge separation and relatively slow charge recombination together with low sensitivity to the stereo-isomeric composition of nanorings, make the [**4**]DHPP⊃C$_{60}$ and [**4**]PP⊃C$_{60}$ systems attractive for photovoltaic applications.

Author contributions

G.G. Investigation, Formal analysis, Writing – original draft, Writing – review & editing

O. A. S. Investigation, Formal analysis, Writing – original draft, Writing – review & editing

A. A. V. Writing – review & editing

A. J. S. Investigation, Supervision, Writing – review & editing

M. S. Supervision, Writing – review & editing, Funding acquisition

Acknowledgements

Conflict of Interests

There are no conflicts to declare.

Data Availability Statement

The data that support the findings of this study are available in the supplementary material of this article.

[1] R. Jasti, J. Bhattacharjee, J. B. Neaton, C. R. Bertozzi, *J. Am. Chem. Soc.* **2008**, *130*, 17646–17647.
[2] H. Omachi, Y. Segawa, K. Itami, *Acc. Chem. Res.* **2012**, *45*, 1378–1389.
[3] S. E. Lewis, *Chem. Soc. Rev.* **2015**, *44*, 2221–2304.
[4] Y. Segawa, A. Yagi, K. Matsui, K. Itami, *Angew. Chem. Int. Ed.* **2016**, *55*, 5136–5158; *Angew. Chem.* **2016**, *128*, 5222–5245.
[5] A.-F. Tran-Van, H. A. Wegner, *Beilstein J. Nanotechnol.* **2014**, *5*, 1320–1333.
[6] D. Lu, Q. Huang, S. Wang, J. Wang, P. Huang, P. Du, *Front. Chem.* **2019**, *7*, 668.
[7] E. J. Leonhardt, R. Jasti, *Nat. Chem. Rev.* **2019**, *3*, 672–686.
[8] D. Wu, W. Cheng, X. Ban, J. Xia, *Asian J. Org. Chem.* **2018**, *7*, 2161–2181.
[9] E. R. Darzi, R. Jasti, *Chem. Soc. Rev.* **2015**, *44*, 6401–6410.
[10] T. Nishihara, Y. Segawa, K. Itami, Y. Kanemitsu, *J. Phys. Chem. Lett.* **2012**, *3*, 3125–3128.
[11] M. Hermann, D. Wassy, B. Esser, *Angew. Chem. Int. Ed.* **2021**, *60*, 15743–15766; *Angew. Chem.* **2021**, *133*, 15877–15900.
[12] J. Wang, X. Zhang, H. Jia, S. Wang, P. Du, *Acc. Chem. Res.* **2021**, *54*, 4178–4190.
[13] Y. Segawa, D. R. Levine, K. Itami, *Acc. Chem. Res.* **2019**, *52*, 2760–2767.
[14] D. Wassy, M. Pfeifer, B. Esser, *J. Org. Chem.* **2020**, *85*, 34–43.
[15] J. S. Wössner, D. Wassy, A. Weber, M. Bovenkerk, M. Hermann, M. Schmidt, B. Esser, *J. Am. Chem. Soc.* **2021**, *143*, 12244–12252.
[16] B. Esser, J. S. Wössner, M. Hermann, *Synlett* **2022**, *33*, 737–753.
[17] K. Ikemoto, S. Yang, H. Naito, M. Kotani, S. Sato, H. Isobe, *Nat. Commun.* **2020**, *11*, 1807.
[18] J. C. Walsh, G. J. Bodwell, *Commun. Chem.* **2020**, *3*, 94–97.
[19] O. A. Stasyuk, A. J. Stasyuk, M. Solà, A. A. Voityuk, *Nanoscale Adv.* **2022**, *4*, 2180–2188.
[20] O. Stephan, P. M. Ajayan, C. Colliex, P. Redlich, J. M. Lambert, P. Bernier, P. Lefin, *Science* **1994**, *266*, 1683–1685.
[21] A. Iida, A. Sekioka, S. Yamaguchi, *Chem. Sci.* **2012**, *3*, 1461–1466.
[22] C. Fujisue, T. Kadoya, T. Higashino, R. Sato, T. Kawamoto, T. Mori, *RSC Adv.* **2016**, *6*, 53345–53350.
[23] J. Usuba, A. Fukazawa, *Chem. Eur. J.* **2021**, *27*, 16127–16134.
[24] G. George, O. A. Stasyuk, A. A. Voityuk, A. J. Stasyuk, M. Solà, *Nanoscale* **2023**, *15*, 1221–1229.
[25] A. J. Stasyuk, O. A. Stasyuk, S. Filippone, N. Martin, M. Solà, A. A. Voityuk, *Chem. Eur. J.* **2018**, *24*, 13020–13025.
[26] A. D. Becke, *Phys. Rev. A* **1988**, *38*, 3098–3100.
[27] C. Lee, W. Yang, R. G. Parr, *Phys. Rev. B* **1988**, *37*, 785–789.
[28] F. Weigend, R. Ahlrichs, *Phys. Chem. Chem. Phys.* **2005**, *7*, 3297–3305.
[29] F. Weigend, *Phys. Chem. Chem. Phys.* **2006**, *8*, 1057–1065.
[30] L. Goerigk, S. Grimme, *Phys. Chem. Chem. Phys.* **2011**, *13*, 6670–6688.
[31] D. R. Lonsdale, L. Goerigk, *Phys. Chem. Chem. Phys.* **2020**, *22*, 15805–15830.
[32] a) L. J. Karas, S. Jalife, R. V. Viesser, J. V. Soares, M. M. Haley, J. I. Wu, *ChemRxiv.* **2023**, 10.26434/chemrxiv-2023-1mnz4; b) D. W. Szczepanik, M. Solà, M. Andrzejak, B. Pawełek, K. Dyduch, M. Kukułka, T. M. Krygowski, H. Szatyłowicz, *J. Comput. Chem.* **2017**, *38*, 1640–1654; c) M. Torrent-Sucarrat, S. Navarro, F. P. Cossío, J. M. Anglada, J. M. Luis, *J. Comput. Chem.* **2017**, *38*, 2819–2828.
[33] J. Kruszewski, T. M. Krygowski, *Tetrahedron Lett.* **1972**, *13*, 3839–3842.
[34] T. M. Krygowski, H. Szatylowicz, J. Dominikowska, M. Palusiak, *Chem. Rev.* **2014**, *114*, 6383–6422.
[35] T. Ziegler, A. Rauk, *Theor. Chim. Acta* **1977**, *46*, 1–10.
[36] F. M. Bickelhaupt, E. J. Baerends, in *Reviews in Computational Chemistry*, (Eds.: K. B. Lipkowitz, D. B. Boyd), Wiley-VCH, New York **1999**, pp. 1–86.
[37] R. F. W. Bader, *Chem. Rev.* **1991**, *91*, 893–928.
[38] T. Yanai, D. P. Tew, N. C. Handy, *Chem. Phys. Lett.* **2004**, *393*, 51–57.
[39] A. Klamt, *J. Phys. Chem.* **1996**, *100*, 3349–3353.
[40] A. A. Voityuk, S. F. Vyboishchikov, *Phys. Chem. Chem. Phys.* **2020**, *22*, 14591–14598.
[41] A. J. Stasyuk, O. A. Stasyuk, M. Solà, A. A. Voityuk, *Chem. Commun.* **2019**, *55*, 11195–11198.
[42] A. J. Stasyuk, O. A. Stasyuk, M. Solà, A. A. Voityuk, *Chem. Commun.* **2020**, *56*, 12624–12627.
[43] O. A. Stasyuk, A. J. Stasyuk, M. Solà, A. A. Voityuk, *J. Nanostructure Chem.* **2022**, 10.1007/s40097-022-00518-w.
[44] O. A. Stasyuk, A. J. Stasyuk, M. Solà, A. A. Voityuk, *ChemPhysChem* **2022**, *23*, e202200226.
[45] J. Ulstrup, J. Jortner, *J. Chem. Phys.* **1975**, *63*, 4358–4368.
[46] A. A. Voityuk, N. Rösch, *J. Chem. Phys.* **2002**, *117*, 5607–5616.
[47] Q. Huang, G. Zhuang, H. Jia, M. Qian, S. Cui, S. Yang, P. Du, *Angew. Chem. Int. Ed.* **2019**, *58*, 6244–6249; *Angew. Chem.* **2019**, *131*, 6310–6315.
[48] A. J. Stasyuk, O. A. Stasyuk, M. Solà, A. A. Voityuk, *J. Phys. Chem. B* **2020**, *124*, 9095–9102.
[49] A. J. Stasyuk, O. A. Stasyuk, M. Solà, A. A. Voityuk, *J. Mater. Chem. C* **2021**, *9*, 9436–9445.
[50] T. Kastinen, D. A. da Silva Filho, L. Paunonen, M. Linares, L. A. Ribeiro Junior, O. Cramariuc, T. I. Hukka, *Phys. Chem. Chem. Phys.* **2019**, *21*, 25606–25625.